Composites Part C: Open Access 18 (2025) 100676

Contents lists available at ScienceDirect

Composites Part C: Open Access

journal homepage: www.sciencedirect.com/journal/composites-part-c-open-access

Effects of resin types on the durability of single yarn polymer composites exposed to hygrothermal environment

Abdullah Iftikhar [a], Allan Manalo [a], Zaneta Senselova [a], Wahid Ferdous [a,*], Mazhar Peerzada [a], Hannah Seligmann [b], Kate Nguyen [c], Brahim Benmokrane [d]

[a] Centre for Future Materials, University of Southern Queensland, Toowoomba QLD 4350, Australia
[b] School of Engineering, Centre for Future Materials, University of Southern Queensland, Toowoomba QLD 4350, Australia
[c] School of Engineering, RMIT University, GPO Box 2476, Melbourne VIC, 3001, Australia
[d] Department of Civil and Building Engineering, University of Sherbrooke, Sherbrooke, Quebec J1K 2R1, Canada

ARTICLE INFO

Keywords:
Hygrothermal ageing
Durability
Glass fibres
Polymer composites
Bio-based resin
Interfacial strength

ABSTRACT

This study evaluated the durability of glass fibre composites prepared using bio-epoxy, vinyl ester and epoxy resin when exposed to a simulated hygrothermal environment. Initially, glass fibre yarns, resins and single yarn composites were exposed to 60oC at 98% relative humidity for up to 3000 h. This was followed by the thermal (DSC), chemical (FTIR), tensile and interfacial shear strength characterization, and the morphological observations under the scanning electron microscope. Results revealed that the resin types significantly influenced the durability of glass fibre yarn composites. Bio-epoxy and vinyl ester resin exhibited thermal stability after exposure to a hygrothermal environment for 3000 h, with an increment of 19oC in the glass transition temperature of epoxy because of the additional cross-linking of the polymeric chain. FTIR spectra reveal that bio-epoxy was chemically stable, while epoxy and vinyl ester resin have undergone chemical degradation because of hydrolysis. The tensile strength of fibre yarn was decreased by 37% because of blistering at the fibre surface, while a reduction of 22%, 10%, and 20% was observed for epoxy, bio-epoxy, and vinyl ester, respectively. Furthermore, the interfacial shear strength was reduced by 15%, 6%, and 25% for epoxy, bio-epoxy, and vinyl ester composites, respectively. Despite the Tg increase, hydrolytic chain scission and damage at the interface reduced the mechanical strength of epoxy. Analytical Hierarchy Process revealed that bio-epoxy resin performed best under hygrothermal conditions when mechanical properties were a priority, whereas vinyl ester resin performed best if physical or thermal properties were most important.

1. Introduction

Fibre-reinforced polymer composites are gaining popularity in building and civil construction [1,2]. In 2023, the composites market was estimated to be worth USD 113.7 billion worldwide and is projected to reach USD 168.6 billion by 2027 [3]. In civil infrastructure, the current applications of composites include building facades [4], railway sleepers [5], bridge decks [6] wind turbine blades [7], marine structures [8] and cross arms in electrical transmission lines [9]. Glass fibres are the predominant choice for these applications [10], owing to their relatively lower cost compared to carbon and basalt fibres. Epoxy resin and vinyl ester resin are most commonly used due to their excellent mechanical, chemical and thermal performance [11]. Rising environmental concerns and awareness about sustainability have led to increased interest in bio-based epoxy resin systems because of their environmental friendliness, biodegradability, non-toxicity, and cost-effectiveness [12,13]. In service conditions, FRP composite structures are most likely to be exposed to harsh environments like solar ultraviolet radiation, elevated in-service temperature [14], moisture, or a combination of them [15]. Exposure to humidity and elevated temperature can lead to significant reversible and irreversible degradation mechanisms [15]. Therefore, a comprehensive knowledge of the

RESEARCH PAPER

* Corresponding author at: Centre for Future Materials, University of Southern Queensland, Toowoomba, QLD 4350, Australia.
E-mail addresses: abdullah.iftikhar@unisq.edu.au (A. Iftikhar), allan.manalo@unisq.edu.au (A. Manalo), zaneta.senselova@unisq.edu.au (Z. Senselova), wahid.ferdous@unisq.edu.au (W. Ferdous), mazhar.peerzada@unisq.edu.au (M. Peerzada), hannah.seligmann@unisq.edu.au (H. Seligmann), kate.nguyen@rmit.edu.au (K. Nguyen), brahim.benmokrane@usherbrooke.ca (B. Benmokrane).

https://doi.org/10.1016/j.jcomc.2025.100676

Available online 30 October 2025

durability and long-term behaviour of composite materials subjected to hygrothermal conditions is essential for their widespread applicability.

The mechanical properties in FRP composites can be considerably reduced because of the internal stresses in the polymer resin caused by moisture absorption [16]. Moisture uptake can cause the fibre/matrix debonding, physical changes, and chemical changes because of the interactions between resin and the water molecules [17]. Moisture diffusion can cause plasticization of resin, which is a reversible mechanism, and hydrolysis of resins, which is an irreversible chemical change responsible for permanent damage. Guo et al [17] reported that the degradation of the interfacial shear strength of carbon/glass composite rods was attributed to the reversible plasticization of the resin, which recovered after desorption, and irreversible debonding at the interface. Sirimanna et al [14]. noted that the exposure to high service temperature (up to 61 °C) has compromised mechanical properties and long-term durability. Similarly, Khotbehsara et al [18] found that elevated temperatures cause matrix softening in epoxy-based polymers, resulted in reduced mechanical performance. Manalo et al [19] reported the reduction of flexural strength, interlaminar shear strength, and stiffness in GFRP composites with vinyl ester resin after exposure to elevated temperature, where the resin could no longer effectively hold the fibres together. Additionally, Hota et al [20] tested GFRP laminates with vinyl ester resin at elevated temperature and reported the weakening of interlaminar shear strength (ILSS) because of the thermal expansion and cracking at the interfacial region of fibre and resin. The increased temperature accelerates the moisture diffusion, causing more severe damage to composites [21,22]. High temperatures not only accelerate moisture ingress but also increase the rate of moisture diffusion, resulting in irreversible changes in polymer matrices, such as debonding failure of the interfacial zone [23]. Scida et al [24] reported that at 90 % relative humidity, flax/epoxy composites exhibited a significant increase in the rate of diffusion after increasing the temperature from 20 °C to 40 °C. Likewise, Ray [25] observed that at 95 % humidity, the increment of temperature from 60 °C to 70 °C resulted in enhanced moisture absorption in glass/epoxy composites due to a higher diffusion rate. Elarbi and Wu [26] concluded that polymer matrices were more adversely affected when subjected to moisture and temperature together compared to only moisture exposure. Among fibres, matrix, and the interface between them, the interface is the most vulnerable part in FRP composites [27] because it is the transition zone between fibre and resin, and all the stresses are transferred through this component [28]. The interface is a complicated as well as a critical component of FRP composites because the interfacial bonding between fibre and resin has a critical influence on the properties of FRPs [29]. Almeida et al [30] observed 38 % reduction in modulus and 30 % decrement in shear strength of carbon fibre/epoxy composites, after exposure at 80 °C and 90 % humidity for 60 days. Moudood et al [31] reported that the saturation of composites of flax and bio-epoxy led to 57 % decrement in modulus and 9 % in tensile strength. This decrease was referred to fibre swelling, fibre/matrix debonding, and resin hydrolysis. Assarar et al [32] reported the degradation in epoxy composites with flax and glass under water ageing was initially matrix dominant, but prolonged immersion resulted in fibre matrix debonding, and once the composite is saturated, the fibre failure came into action. The governing failure mechanism for both the composites after water ageing was identified to be fibre-matrix interface weakening. Nikforooz et al [33] used a single fibre fragmentation approach to investigate the fibre/matrix interface and demonstrated that fibre sizing significantly influenced the interfacial strength and debonding at the interface. Zhong et al [34] exposed the GFRP and CFRP composites to the hygrothermal environment at 80 °C and stated that carbon FRP (CFRP) performed better and retained 95.75 % strength, whereas GFRP composites retained only 74.65 % of their original strength. Furthermore, they observed a 29.7 % strength reduction in glass fibres after hygrothermal exposure and declared it as the core cause of the strength reduction of GFRP composites. Krauklis et al [15] concluded that plasticization in the epoxy matrix, degradation of the interface and degradation of the glass fibre surface were the underlying mechanisms responsible for the reduced performance of DFRP composites after hygrothermal ageing. There are several models in previous literature to predict the durability performance of fibre-reinforced composites when exposed to different aggressive environments. The most frequently used approach to predict the moisture diffusion process is the one-dimensional Fickian model [24,31]. The Arrhenius prediction model is widely used by researchers for the lifetime prediction of polymers exposed to different environments [17,20]. Dong et al [35] developed an artificial neural network-based model using 272 durability datasets to predict the long-term tensile strength of GFRP bars under alkaline exposure.

Despite various studies available, there is inconsistency and disagreement in the identified role of constituent material, i.e., fibres, resin, and the interface, on the durability of FRP composites. Some studies reported that the matrix is the only constituent being affected [23,25,30], while some studies indicated that the damage at the interface between fibre and resin is the major contributor to the degradation [32,36]. Zhong et al [34] referred the degradation in FRP composites to the reduction of tensile strength of fibres after hygrothermal ageing. On the contrary, all three constituents were reported to be affected and contribute to the degradation [7,15,24,25]. Furthermore, it has been reported that the synthetic fibres have very low water absorption, while a considerable reduction in the strength of these fibres was identified after hygrothermal exposure [34]. It is important to note that these discrepancies are caused by the lack of quantification on the role of each constituent material, and available studies focused on a specific resin system. Additionally, research studies available on single fibre or single yarn composites evaluated the interfacial strengths of non-exposed samples. Therefore, a systematic and thorough investigation is required to identify the contribution of fibre, resin and the interface, in the degradation of polymer composites with various resin types and glass fibres subjected to a hygrothermal environment.

This study implemented an extensive accelerated ageing program to analyse the durability of glass fibres, resin systems, and single glass yarn composites under the synergistic effect of moisture and temperature. The study focused on characterizing the physical, mechanical and microstructural characteristics of constituents of glass fibre composites after exposure to elevated in-service temperature of 60 °C, relative humidity of 98 % up to 3000 h. The novelty of this research resides in its comparative and comprehensive approach, where multiple resin systems; epoxy, bio-epoxy and vinyl ester, are evaluated under identical accelerated hygrothermal ageing conditions. A better understanding of degradation is obtained at the material component level by separately assessing the properties of the glass fibres and resin matrix. The optimal resin system that can minimise the impact of the hygrothermal condition on the durability of glass fibre composites was identified by the analytical hierarchy process (AHP). The outcome of this research will provide systematic and in-depth information about the effect of resin types and the contribution of constituent materials in the degradation mechanism of polymer composites under long-term hygrothermal exposure for their safe and effective use in building and civil engineering construction exposed to harsh service environments.

2. Materials and experimental program

2.1. Materials

A 68 Tex (gm/km) E-glass fibre yarn supplied by Colan Australia, and three different resin systems (bio-epoxy, vinyl ester, and epoxy) were utilized to have three different variations of fibre/matrix interfaces. E-glass fibres were coated with universal silane-based special sizing, which is directly compatible for use in epoxy and vinyl ester resins and ensures fast impregnation with resin systems. The diameter and volumetric density of glass fibre yarn were 189.7 μm and 2.54 g/cm^3, respectively. A Prime 27 epoxy (DGEBA, Bisphenol A diglycidyl ether) infusion

system with high glass transition (T_g) hardener (mix ratio: 100:25 by weight) was used. Also, a two-part, non-toxic, aliphatic bio-epoxy with glycerol core (mix ratio: 77:23 by weight) was supplied by Change Climate Pty Ltd. Likewise, SPV6036 vinyl ester infusion resin (epoxy-Bisphenol A-based) with a special cumene hydroperoxide-based catalyst (mix ratio:100:1.5 by weight) supplied by Allnex, was used. The basic parameters of the resins provided by the supplier are presented in Table 1. A two-part (1:1) liquid silicon was also used to fabricate the special flexible moulds for easy sample manufacturing.

The bio-based epoxy resin used in this study differs fundamentally from the conventional DGEBA epoxy in both composition and molecular architecture. Bio-epoxy resin is an aliphatic epoxy derived from a renewable, biological glycerol core, completely free from bisphenol-A. In contrast, conventional diglycidyl ether of bisphenol-A (DGEBA) epoxy is based on aromatic Bisphenol A (BPA) backbone.

2.2. Specimen preparation

Neat resin samples with dog-boned shapes were manufactured with specific dimensions, illustrated in Fig. 1(a and b). Properly mixed resin was poured into specially prepared silicone moulds, as shown in Fig. 1 (c). Curing was carried out following the manufacturer's recommendations (summarised in Table 2), to have a comparative assessment of durability under standard usage conditions. For the single yarn fragmentation test, dog-bone-shaped single yarn composites similar to neat resin samples were manufactured by combining fibre yarn and three different resin systems. Initially, fibre yarns were centrally aligned with the help of guide notches engraved exactly at the central axis of the sample, in the manufactured silicon moulds, as shown in Fig. 1(a). The yarns were seated in the guide notches at both ends and held under light tension by hanging small weights (~5 g) on each side to remove sag and make the alignment straight. After alignment, glue was poured into the notches at both ends to seal the edges and eliminate the resin leakage during manufacturing. The weights were removed after setting the glue, followed by the mixing of part A and part B of the resin and pouring into silicone moulds using a 50 ml syringe. Fig. 2(b and c) shows fully cured neat resin and single yarn composite specimens. Specimens were carefully prepared to minimise any air bubbles. It was also observed that although a few specimens contained occasional sub-millimeter bubbles, these were isolated, not making a connected network that can facilitate connected porosity or intersecting the interface. So, they would not create moisture transport pathways and their influence on the durability was considered negligible. To ensure consistency and eliminate variations, all samples were prepared in a single continuous run under similar conditions.

2.3. Hygrothermal conditioning

The simulated hygrothermal condition was accomplished by exposing the samples in an environmental chamber (Weiss-Voetsch C4–340) capable of maintaining a set temperature and humidity level. Glass fibre yarn, neat resin samples and single yarn composites were separately placed in the environmental chamber under controlled environment at 60 °C and 98 % relative humidity for a period of 1000hr, 2000hr, and 3000hr as shown in Fig. 2(d). These temperature and humidity levels were selected to simulate accelerated hygrothermal ageing while also representing the actual in-service temperature [14] that a composite may experience during its service life. Although the exposure temperature exceeds the curing temperatures of epoxy and bio-epoxy, this study is focused solely on comparing their durability under standard manufacturing parameters and realistic in-service conditions. Eight samples (five for mechanical testing and three for thermal/chemical and microstructural testing) for each resin type were exposed to conditioning for one exposure duration.

Table 1
Physical properties of uncured resins.

Raw Material	Density (g/cm^3)	Viscosity at 25 °C (cP)		
		Resin Part	Hardener	Initial mixed system
Epoxy	1.11–1.13	480–510	25–27	310–330
Bio-Epoxy	1.150–1.155	750–850	15–20	150–250
Vinyl Ester	1.04–1.06	300–350	20–23	220–270

2.4. Physical and mechanical testing

Physical testing involves moisture absorption and observation of the changes in colour after exposure to hygrothermal conditioning. The colour change was visually inspected and quantified by calculating the yellowing index of each resin type after 1000 hr, 2000 hr, and 3000 hr with the help of high-resolution images acquired using an Olympus DX100 microscope. The moisture absorption was measured during the exposure of samples according to ASTM D570–22 [37]. The central portion of the dog-bone sample, with a uniform width resembling a rectangular sample, was cut and used for water absorption measurements. The excess water was removed by wiping off the surface with a cotton towel, and the samples were weighed on an electronic balance with a tolerance of 0.0001 g.

ASTM C1557–20 [38] was used for the tensile strength evaluation of glass fibre yarn. The similar test procedure that also adopted by Seghini et al [27] for flax yarns extracted from Biotex 2 × 2 twill fabric (200 g/m^2). Fibre yarns were mounted on paper tabs with adhesive at both ends, with a gauge length of 33 mm, as shown in Fig. 2(a) and tested under displacement control using a TA. XTplus100C texture analyzer with 1 kN load cell and a crosshead rate of 1 mm/min, as illustrated in Fig. 3(a-b). The testing of resin samples was carried in a 10 kN MTS Alliance testing equipment at a test speed of 1mm/min, following ASTM D638–22 [39], (Fig. 3c). Likewise, the same test setup (Fig. 3d) and testing speed was set for the single yarn fragmentation test for calculating interfacial shear strength (IFSS) values. A laser extensometer was used during each tensile test to record the strain up to failure. At least 5 samples from each resin type after each exposure duration were tested to get consistent and reliable results. Table 3 summarizes the tests, along with the relevant standard and number of samples.

2.5. Chemical and thermal analysis

The chemical changes in the functional groups were detected by FTIR analysis after each exposure duration. Nicolet iS50 FTIR spectrophotometer was used for the collection of FTIR spectra across the spectral range of 400–4000 cm^{-1}. The samples were dried the in an oven for 16 h at 60 °C before performing FTIR. The samples were then stored in a desiccator for 7 days for further dehydration to minimise the influence of moisture, thereby enhancing the reliability of FTIR spectra. Differential scanning calorimetry was employed following ASTM D3418–21 [40], for the determination of glass transition temperature (T_g). For determining T_g, a cured resin sample between 10 and 15 mg was accurately weighed using a sensitive balance, placed in a standard SDT aluminium pan and transferred to a TA DSC 25 instrument. The DSC was performed at a heating rate of 10 °C/min, up to 150 °C using a 200 ml/min purge gas (N_2). Three samples for each resin type were analysed after each exposure duration. Likewise, DSC was employed to measure the level of curing for each resin system. The uncured resin sample was placed in the DSC pan, and the total heat of reaction was obtained from exothermic peaks up to a temperature of 300 °C at a heating rate of 10 °C/min. Similarly, 10 to 15 mg of cured resin was placed in the pan to calculate the residual heat of reaction. The difference in the enthalpies of uncured and cured resins was used to calculate the degree of cure.

2.6. Microscopic observations

JEOL JCM-6000 (SEM) was used to reveal any damage to the fibre

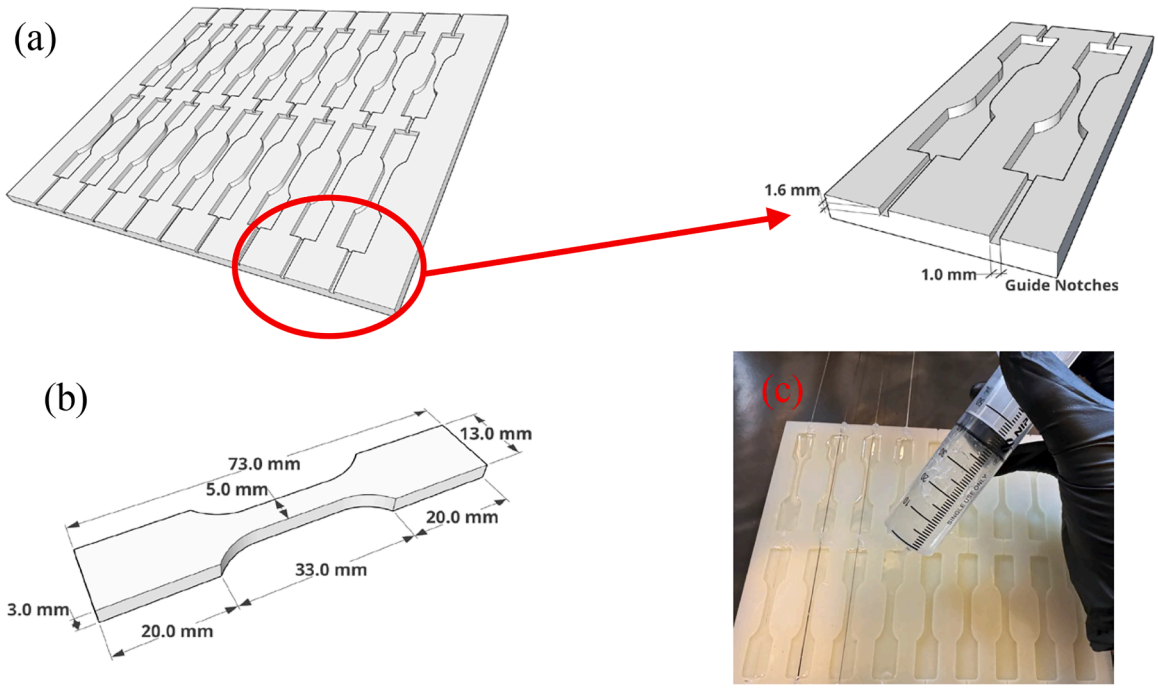

Fig. 1. (a) Silicone mould, (b) Sample geometry, (c) Resin pouring.

Table 2
Curing time and temperature.

	Curing Time	Curing Temperature
Bio-Epoxy	7 days	Room temperature
Epoxy	24 hrs	Room temperature
	16 hrs	50 °C
Vinyl Ester	24 hrs	Room temperature
	2 hrs	120 °C

and interfacial zone of fibre and resin after exposure to hygrothermal environment. The samples taken from the specimens tested for the IFSS were cut to a thickness of 3 mm, fixed on an aluminium plate, and then gold-plated with a 10 nm layer to eliminate the charging effect.

3. Results and discussion

3.1. Effect of hygrothermal exposure on physical properties

3.1.1. Water absorption

The water absorbed by each resin type was calculated by measuring the increase in mass after different time intervals. The percentage absorption was determined using Eq. (1).

$$Absorption\ (\%) = \frac{W_s - W_d}{W_d} x100 \quad \text{(Eq. 1)}$$

where W_s is the saturated weight and W_d is the dry weight.

The water absorption of resin samples under hygrothermal conditioning over time is shown in Fig. 4(a). The normalised moisture uptake to provide a dimensionless comparison of the rate of moisture uptake relative to the material's capacity is exhibited in Fig. 4(b). An average value of three specimens of each resin system with a coefficient of variance of less than 5 % was used. After exposure to 60 °C and 98 % RH, epoxy, bio-epoxy, and vinyl ester resins exhibited the maximum water absorption of 2.01 %, 9.55 %, and 0.65 %, respectively, after 3000 h as presented in *Table 4*.

Among the three, bio-epoxy resins, derived from renewable sources, tend to absorb more water compared to traditional petroleum-based epoxies. It has shown the highest water absorption, absorbing five times more water compared to epoxy and 15 times more than vinyl ester resin. This increased water absorption is primarily due to their chemical structure and the presence of hydrophilic functional groups. Bio-epoxy resins often contain hydroxyl (-OH) and carboxyl (-COOH) groups from their natural feedstocks. These polar groups have a strong affinity for water molecules, leading to higher moisture uptake. Compared to conventional epoxies, bio-epoxies may have a lower crosslink density.

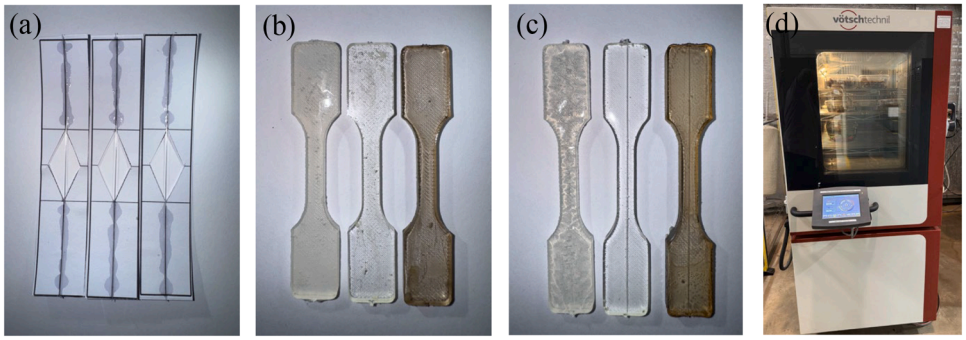

Fig. 2. (a) Glass Fibres (a) Neat resin samples (c) Single yarn composites (d) Simulated hygrothermal exposure in an environmental chamber.

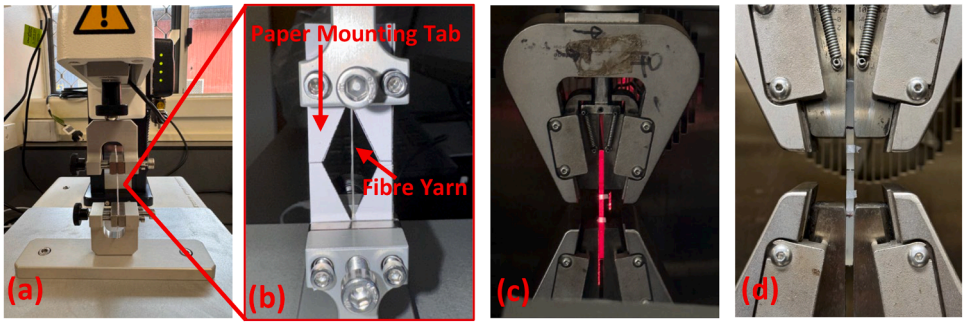

Fig. 3. Testin configuration for (a, b) Tensile test of fibre yarn, (c) Tensile test of neat resin, (d) Single yarn fragmentation test.

Table 3
Sample counts and test standards for each resin system.

Properties	Test Standard	Number of Samples			
		0h	1000h	2000h	3000h
Physical Properties					
Water Absorption	ASTM D570 –22 [37]	3	3	3	3
Colour Change		3	3	3	3
Differential Scanning Calorimetry (DSC)	ASTM D3418 –21 [40]	3	3	3	3
Tensile Properties					
Fibre Yarns	ASTM C1557 –20 [38]	5	5	5	5
Neat Resins	ASTM D638 –22 [39]	5	5	5	5
Interfacial Shear Strength (IFSS)		5	5	5	5
Fourier Transform Infrared Spectroscopy (FTIR)		3	3	3	3
Scanning Electron Microscopy (SEM)		3	3	3	3

This less compact network allows water molecules to penetrate more easily into the polymer matrix. In addition, the irregular arrangement of polymer chains in bio-epoxies creates free volume, facilitating water diffusion throughout the material [41]. Another possible reason could be the presence of a glycerol core, unlike the conventional Bisphenol A (BPA) core in the case of epoxy and vinyl ester, which has a molecular formula $C_3H_8O_3$. The glycerol with three hydroxyl groups has high chances of hydrogen bonding with water, so it is hygroscopic, enabling bio-epoxy to absorb more water compared to other resin systems. Contrary to this, vinyl ester has shown the highest resistance to water absorption. Although both vinyl ester resin and epoxy resin share a similar Bisphenol A core but in vinyl ester, reduced surface exposure of the core minimised the chances of hydrogen bonding with water molecules because of reduced availability of hydroxyl groups.

The rate of water diffusion in resin systems was calculated using the Fickian diffusion analytical model as adopted by previous researchers [24,31]. Water absorption measurements were restricted to the central gauge length of the dog bone samples to ensure the one-dimensional water diffusion behaviour. The middle part with uniform geometry was physically cut and exposed for water absorption. For the samples with uniform thickness, Fickian law can be represented by Eq. (2) [42].

$$\frac{M_t}{M_\infty} = 1 - \frac{8}{\pi^2}\sum_{n=0}^{\infty}\frac{1}{(2n+1)^2}exp\left[-\frac{(2n+1)^2\pi^2 D_t}{h^2}\right] \quad \text{(Eq. 2)}$$

In this equation, $M\infty$ is the total weight of absorbed water at full saturation, M_t represents the water absorbed at a given time t, summation index is represented by n, geometry in terms of thickness is denoted by h, and D_t is the diffusion coefficient. Shen and Springer [43] have resolved the equation into two parts. For $M_t/M_\infty < 0.6$, the expression is reduced to Eq. (3):

$$\frac{M_t}{M_\infty} = \frac{4}{h}\sqrt{\frac{D_t}{\pi}} \quad \text{(Eq. 3)}$$

For $Mt/M\infty > 0.6$, it can be expressed as Eq. (4):

$$\frac{M_t}{M_\infty} = 1 - exp\left[-7.3\left(\frac{D_t}{h^2}\right)^{0.75}\right] \quad \text{(Eq. 4)}$$

The average diffusion coefficient can be expressed as Eq. (5):

Table 4
Comparison of moisture uptake (wt %) for the three neat resins at different durations.

Neat resin	Water absorption (%)		
	1000 hr	2000 hr	3000 hr
Epoxy	1.9137	1.9738	2.0152
Bio-epoxy	8.6994	9.3113	9.5584
Vinyl ester	0.5782	0.5891	0.6539

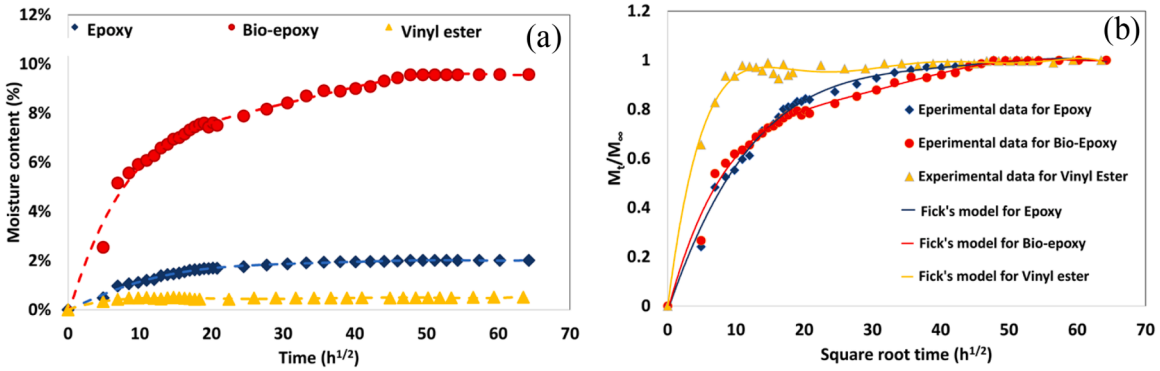

Fig. 4. (a) Moisture absorption after hygrothermal exposure. (b) Water uptake curve using experimental data and analytical model after hygrothermal exposure.

$$D = \pi\left(\frac{kh}{4M_\infty}\right)^2 \quad \text{(Eq. 5)}$$

In Eq. (5), k represents the slope of the initial linear region ($M_t/M_\infty < 0.6$) of M_t/M_∞ versus $\sqrt{t}$ plot. Fig. 4(b) shows the comparison of experimental and Fickian behaviour of all three resins. All the samples showed an initial linear region, followed by decreased absorption, and finally, a level of full saturation was achieved. These findings align with those reported by Moudood et al [31] and Assarar et al [32] in their research. Although vinyl ester absorbs the least moisture at saturation, it reaches saturation faster than epoxy or bio-epoxy, as demonstrated in Table 5 and Fig. 4(b). Vinyl ester has the fastest rate of water diffusion with a steeper initial slope and a diffusion coefficient of 8.57×10^{-6} mm^2/s and reached the saturation level after 150 h of exposure. Bio-epoxy resin showed a relatively slow rate of diffusion compared to vinyl ester and reached the saturation level after exposure for 2200 h with a diffusion coefficient of 2.14×10^{-6} mm^2/s. The slowest water diffusion was exhibited by epoxy with a diffusion coefficient of 1.43 mm^2/s and full saturation after 2500 h of hygrothermal exposure. These results indicate that both the water uptake and diffusion rate are largely influenced by the selected type of resin. Vinyl ester exhibited the highest water resistance but allows rapid diffusion, while regular epoxy provides intermediate water absorption with the slowest diffusion rate.

3.1.2. Change in colour

After hygrothermal exposure, the resin systems have shown a significant change in colour, as shown in Fig. 5. The yellow colour became darker with increased exposure duration, and the maximum yellowing effect was observed after 3000 h. Although small pitting can be observed at the surface due to erosion of resin in the case of bio-epoxy and vinyl ester, there were no visible cracks on the surface, as shown in Fig. 6. The yellowing index of all the resins before and after exposure to 3000 h was calculated using the formula recommended by ASTM E313–20 [44], expressed as Eq. (6).

$$YI = \frac{100(1.28X - 1.06Z)}{Y} \quad \text{(Eq. 6)}$$

In this expression the tristimulus values are represented by X, Y, and Z in "CIE XYZ" picture space, and YI is the yellowness index. The tristimulus values were measured by applying MATLAB code to extract the X, Y and Z values from RGB pictures taken in the polarized mode of the Olympus DX100 microscope at the same magnification levels.

Fig. 6 shows that the bio-epoxy resin exhibited maximum yellowness intensity, followed by epoxy resin, with their yellowing index increased by 67.97 and 46.01 points, respectively, as presented in Table 6. The chromophores, such as $C = C$ bonds and carbonyl groups ($C = O$), were responsible for the yellowing of resin systems, as also reported by Chao Wu et al [45]. Both epoxy and bio-epoxy contain $C = C$ (Section 3.3), which was responsible for yellowing because of radical oxidation of chromophores after exposure. On the other hand, vinyl ester has a carbonyl group ($C = O$) as well, in addition to $C = C$ (Section 3.3), which also explains the light-yellow colour and a higher yellowing index of 47.54, even before exposure [46]. It can also be observed from Fig. 5 and Table 6 that vinyl ester has shown better yellowing resistance as compared to epoxies, with an increment of only 7.47 points in YI, because ester linkages in vinyl ester are fewer in number and sterically shielded by its hydrophobic epoxy core. While both DGEBA epoxy and vinyl ester use bisphenol-A backbones, in vinyl esters, the aromatic rings are terminated by methacrylates at the ends of the polymeric chain after esterification, reducing their surface accessibility during hydrothermal ageing compared to recurring aromatic units in epoxy. Additionally, vinyl ester absorbs less moisture (0.65 %), minimizing swelling stresses that accelerate oxidative yellowing. The observed yellowing mechanism reflected the occurrence of chemical changes because of oxidation and the formation of chromophores. However, the change in colour alone cannot confirm whether these chemical changes resulted in degradation. Therefore, we interpreted these chemical changes with FTIR in Section 3.3 to determine whether these reactions resulted in the degradation of resins because of hydrolysis or oxidation. For applications where aesthetics is important, yellowing may remain a practical limitation even when mechanical integrity is largely retained.

Table 5
Diffusion coefficient of resin systems.

Materials	Diffusion Coefficient ($Dx10^{-6}$) mm^2/s	Time to saturation (hrs)
Epoxy	1.43	2500
Bio-epoxy	2.14	2200
Vinyl ester	8.57	150

3.2. Effect of hygrothermal exposure on thermal properties

Three samples of each resin system, weighing 10–15 mg after each exposure duration, were analysed using DSC to observe the changes in T_g and degree of cure after hygrothermal exposure.

3.2.1. Degree of cure

The degree of cure is one of the key parameters to ensure that the optimum curing has been achieved under specified conditions before the mechanical evaluation of resins. The degree of cure of resins was evaluated by differential scanning calorimetry (DSC) using the residual reaction enthalpy. The enthalpy of uncured resin was measured by calculating the area under the curve of the exothermic peak obtained from DSC. Following that, the enthalpy of cured resin was calculated through the area under the exothermic portion. To calculate the degree of cure, the enthalpy of full cure (i.e., obtained from an exothermic peak of uncured resin) and the enthalpy of residual cure (i.e., difference between uncured and cured resin) were used. The formula used for the calculation is given as Eq. (7) [47]:

$$\%\ Cure = \frac{\Delta H_T - \Delta H_R}{\Delta H_T} X100 \quad \text{(Eq. 7)}$$

where, total enthalpy of uncured resin is denoted by ΔH_T and enthalpy of fully cured resin was represented by ΔH_R.

It can be inferred from Table 7 that all the resins were fully cured and the hygrothermal exposure for 3000 h has not affected their degree of cure.

3.2.2. Glass transition temperature (Tg)

Table 8 summarizes the variation in T_g of resins after exposure to hygrothermal environment. The bio-epoxy exhibited the lowest Tg of 44.4 °C before exposure, and a slight increment of 5 % was noted after exposure for 3000 h. Vinyl ester resin showed the highest Tg value of 103.6 °C and exhibited thermal stability without any further increase after exposure for 3000 hrs. It can also be observed from Table 8 that the epoxy resin had a T_g of 73.4 °C before exposure. This has increased progressively with increasing exposure time, with an increment of 26 % after 3000 hr. This increment was attributed to the additional cross-linking at elevated temperatures due to residual reactive groups, oxidation, or catalyst activation [16]. The increase in T_g in epoxy resin under hygrothermal exposure can be referred to the secondary cross-linking facilitated by multiple hydrogen bond formation with the polymeric chains of resin because of Type-II bound water [16]. Furthermore, the reduced free volume due to the rearrangement of polymer chains through thermal annealing enhanced the secondary bonding and eventually increased Tg. A similar trend of increased T_g of epoxy resin after prolonged exposure to hygrothermal ageing was also observed by Zhou and Locus [48]. Likewise, the T_g of bio-epoxy was slightly increased after exposure as Type-II water has facilitated the secondary cross-linkage. Despite the highest water uptake, the increase in Tg was limited to only 5 % because of the dominance of Type-I water.

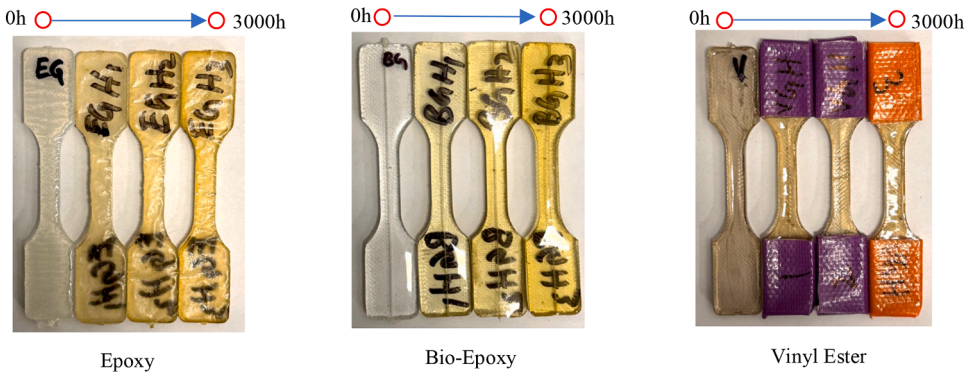

Fig. 5. Yellowing of resin systems after hygrothermal ageing.

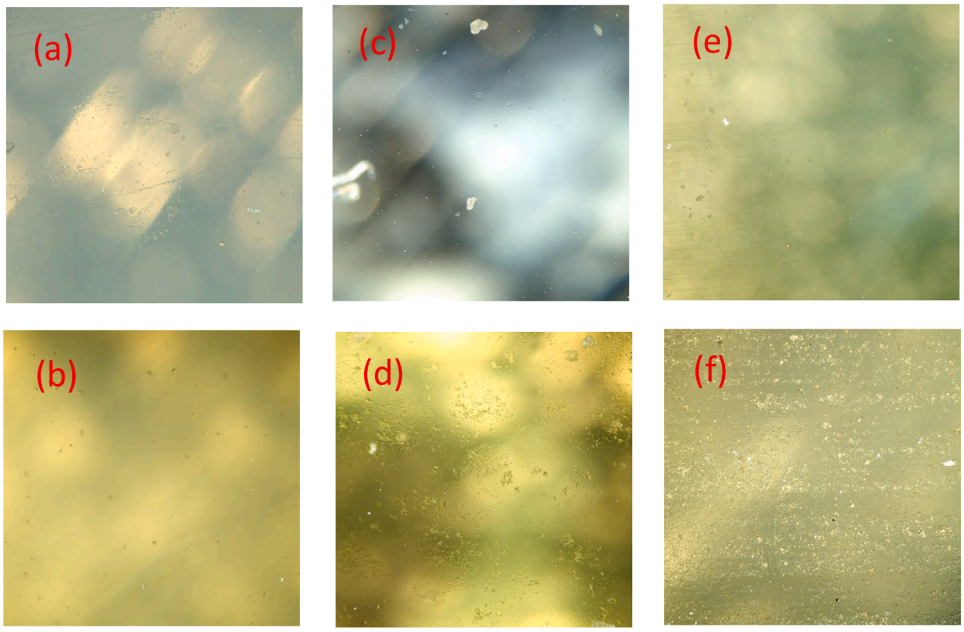

Fig. 6. Microscopic images (a) unexposed epoxy, (b) exposed epoxy, (c) unexposed bio-epoxy, (d) exposed bio-epoxy, (e) unexposed vinyl ester, (f) exposed vinyl ester.

Table 6
Yellowing index of resins after hygrothermal conditioning.

Resin Types	Yellowing Index		Difference in YI
	Control	3000 h	
Epoxy	25.33	71.34	46.01
Bio-epoxy	6.47	74.44	67.97
Vinyl ester	47.54	55.01	7.47

In bio-epoxy, the additional hydroxyl groups have a high tendency of hydrogen bonding with water, but most of the absorbed water remained as Type-I bound water, which was lost when the specimens were stored at room temperature. In contrast, vinyl ester was thermally stable without any increase in Tg after exposure because of very small water absorption (0.65 %) and high Tg value (103.6 °C) before exposure, which was significantly higher than the exposure temperature.

3.3. *Effect of hygrothermal exposure on the chemical properties*

FTIR analysis was performed on resin samples to identify their chemical composition in terms of functional groups. In all three resin types, O—H and C—H were the major phases in the FTIR spectra. Fig. 7 (a-c) shows that the intensities of peaks differ, but the number of peaks and their corresponding wavenumber are similar for unexposed and exposed samples. In the case of epoxy resin (Fig. 7a), the absorption band at 3390 cm^{-1} reflects O—H stretching. The second peak at 2920 cm^{-}

Table 7
Degree of cure for each resin system.

Resin Type	ΔH_T (J/g)	ΔH_R (J/g)				% Cure			
		Control	1000 hr	2000 hr	3000 hr	Control	1000 hr	2000 hr	3000 hr
Epoxy	420.28	0.0321	0.0288	0.0267	0.0245	99.99	99.99	99.99	99.99
Bio-Epoxy	262.79	0.1041	0.0325	0.0269	0.0150	99.96	99.98	99.99	99.99
Vinyl Ester	345.34	0.0577	2.0567	0.0317	0.0299	99.40	99.98	99.99	99.99

Table 8
Glass transition temperature Tg (°C) and retention after hygrothermal exposure.

Resin Type	Glass Transition Temperature (°C)				T_g retention after 3000 hrs
	Control	1000 hrs	2000 hrs	3000 hrs	
Epoxy	73.45	89.85	91.76	92.52	126 %
Bio-epoxy	44.49	44.24	47.56	46.64	105 %
Vinyl Ester	103.64	102.10	103.20	103.58	100 %

^{1}–2861 cm^{-1} represents the C—H bond of epoxy resin [23]. The bands present at wavenumber 1608 cm^{-1} and 1504 cm^{-1} are the aromatic $C = C$ stretching, which is the characteristic band of DGEBA epoxy systems. Several peaks between wavenumbers 1234 cm^{-1} and 1033 cm^{-1} correspond to epoxide C—O-C ring of an aromatic ether [16,23]. Whereas the band at 830 cm^{-1} refer to the epoxide stretching [49]. In the case of bio-epoxy resin (Fig. 7b), the absorbance peak present at 3394 cm^{-1} represents O—H stretching. A band at 2912 cm^{-1} is assigned to C—H stretching of epoxy systems [23]. Peaks at 1620 cm^{-1} and 1467 cm-1 are assigned to stretching of $C = C$. Band at wavenumber 1087 cm^{-1} is attributed to C—O stretching of aliphatic ether, which refers to the characteristic band for bio-epoxy resin [50].

FTIR spectra of vinyl ester resin (Fig. 7c) are very similar to those of epoxy resin systems. The absorbance peak present at 3436 cm-1 refers to stretching of O—H bond, and that present at 2920 cm-1 represents the stretching of C—H. The band present at wavenumber 1716 cm-1 is assigned to ester $C = O$ stretching [23], and the one at 1636 cm^{-1} corresponds to the acryloyl double bond, which confirms the formation of vinyl ester resin. The peak at 1504 cm-1 represents the aromatic $C = C$ stretching, which refers to the typical band of DGEBA epoxy systems. The peaks between 1234 cm-1 and 1033 cm-1 are attributed to epoxide C—O-C in the case of an aromatic ether [16,23]. These FTIR results provided a good indication of the complete curing and formation of polymeric resin systems.

The chemical degradation in resin systems because of water absorption is mainly due to plasticization and hydrolysis. The hydrolysis reaction is responsible for the generation of additional hydroxyl groups (-OH). The occurrence of the hydrolysis reaction was assessed by calculation of the areas under the O—H region and C—H region located within the range of 3300–3400 cm^{-1} and 2900–3000 cm^{-1}, respectively, as illustrated in Fig. 7(d). The ratio of area under O—H and C—H was calculated afterwards. A similar approach has been used by Benmokrane et al [10] for examining the chemical changes in GFRP bars after exposure to a saline environment. Table 9 shows that O—H/C—H has increased in epoxy and vinyl ester, indicating the formation of new hydroxyl groups after hygrothermal exposure. Mishra and Singh [16] also referred the increase in O—H intensity to the hydrolysis reaction. Whereas the decrement in the O—H/C—H ratio in bio-epoxy indicates no hydrolysis reaction or chemical change after hygrothermal exposure.

Table 9
Ratio of O—H and C—H peaks in FTIR spectra.

O-H/C—H ratio					
Epoxy resin		Bio-epoxy resin		Vinyl ester resin	
Unconditioned	3000 hr	Unconditioned	3000 hr	Unconditioned	3000 hr
0.835	1.15	1.530	1.311	0.754	0.867

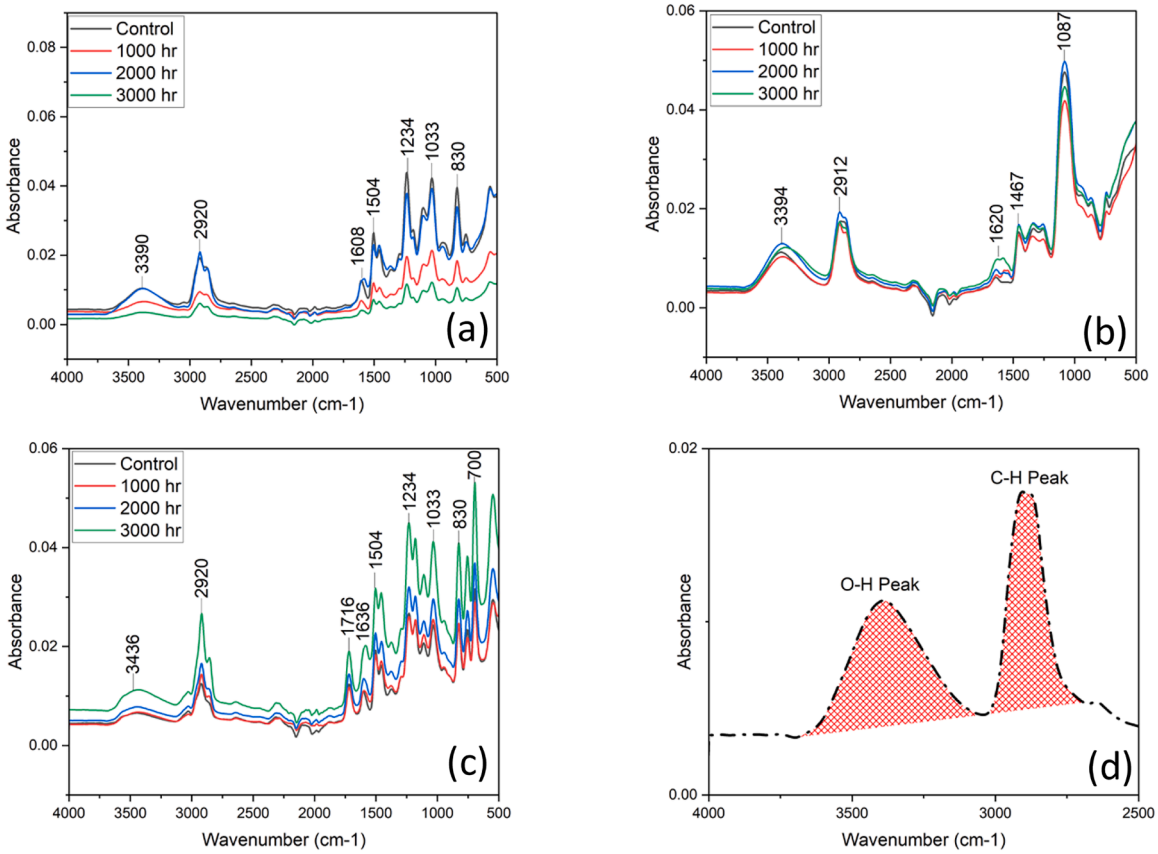

Fig. 7. FTIR analysis (a) Epoxy (b) Bio-epoxy (c) Vinyl ester (d) O—H/C—H peaks.

3.4. Effect of hygrothermal conditioning on tensile properties

3.4.1. Tensile strength of glass fibres

Table 10 summarizes the reduction in tensile strength of glass fibre yarn after exposure. The average diameter of fibre yarn was 189 μm, calculated by the average volumetric density and weight of a specific length of yarn of five samples. A strength reduction of almost 37 % was noticed in glass fibre yarn after 3000 h of direct hydrothermal exposure, as presented in Table 10. The major cause of strength reduction could be the chemical degradation of the sizing layer because of the hydrolysis of siloxane (Si-O-Si) bonding. The sizing has an important role in maintaining adhesion between the fibres within the multifilament yarn, so the yarn acts as a single coherent body. Once the sizing layer was damaged because of exposure, the adhesion between the fibres in the yarn was reduced, and the yarn exhibited a progressive failure at lower loads. Similar findings were observed by Zhong et al [34] where they stated a 29.7 % decrement in the tensile properties of E-glass fibres after immersion in water at 80 °C for 38 days and attributed it to the defects in the sizing layer. Likewise, Nikforooz et al [33] identified a 42 % reduction after conditioning at 70 °C for four weeks and attributed it to the degradation of the sizing layer of glass fibres after hygrothermal exposure resulted in a weaker interface and debonding. Various researchers have reported that the degradation of silane-based sizing layer occurs because of the hydrolysis of Si-O-Si bonding when exposed to elevated temperatures and hygrothermal conditions [33]. The degradation of the sizing layer and loss of protection eventually resulted in the significant strength loss in glass fibres. Thomson et al [51] further clarified that loss of sizing layer is not the only reason for strength loss; damage in the glass fibre itself also exists after the sizing layer has been removed. This reduction in strength could directly affect the integrity of glass fibre composites in aggressive environments. In FRP composites, the fibre is less sensitive to high temperature and humidity because of a protective layer of the resin systems [21]. However, water can still penetrate and reach the fibres after prolonged exposure, potentially compromising the mechanical strength significantly.

The surface deterioration of the fibres because of hygrothermal ageing was analysed by SEM micrographs. It can be observed from Fig. 8 that before exposure, the glass fibres had a very smooth surface and regular shape, but after being exposed for 3000 h, an uneven and rough surface can be observed because of excessive damage to the sizing layer due to moisture and elevated temperature. Blistering can be observed at the surface that can eventually result to the removal of the sizing layer after bursting, and surface cracking might occur, that could be responsible for the loss of strength of fibres.

3.4.2. Tensile strength of neat resin

Tensile strength results of resin systems before and after exposure are presented in Table 10. Unexposed epoxy resin achieved a maximum strength of 62.4 MPa, which is in line with that documented by Seghini et al [27]. Likewise, a tensile strength of 52.32 MPa was measured for bio-epoxy resin before exposure, similar to that reported by [52]. The lowest strength was measured for vinyl ester resin, i.e., 40.70 MPa, which is close to that reported by Seghini et al [27]. The tensile strength was reduced progressively after exposure to hygrothermal condition in the case of epoxy and bio-epoxy as presented in Table 10. While in the case of vinyl ester, the strength increased initially because of some additional cross-linking of polymeric chains, but after prolonged exposure, the strength was significantly reduced at 3000 h. A strength loss of 18.43 %, 9.69 % and 16.95 % was exhibited by epoxy, bio-epoxy, and vinyl ester resin, respectively, after hygrothermal exposure for 3000 hrs.

The major reason for the strength reduction of the resin system could be plasticization and/or hydrolysis due to water absorption [36]. Elevated temperature has increased molecular mobility, making resins more sensitive, resulting in moisture absorption [23]. Moisture diffusion resulted in swelling and internal stresses that led to the micro-cracks. Those cracks served as paths for ingress of water molecules, ultimately causing plasticization of the resin [3,15]. The hydrolysis caused by the interaction of hydroxyl groups with the polar sites in polymeric chains of resin was also responsible for the strength loss. In epoxy resin exposed to elevated temperature and moisture, an increment in Tg was observed along with increased moisture uptake, most probably due to the additional cross-linking facilitated by type-II bound water. However, a considerable decrement in tensile strength was noticed after 3000 h, which might be attributed to plasticization and hydrolytic effects, confirmed by the increased O—H/C—H ratio in FTIR spectra. The strength reduction in vinyl ester after exposure is lower compared to epoxy because of minimal water uptake and thermal stability with no change in Tg. Hydrolysis of vinyl ester was evident from FTIR analysis, responsible for the strength loss, but the extent of hydrolysis was less compared to epoxy resin. The bio-epoxy resin with the highest water uptake among the three systems has exhibited thermal stability and, interestingly, exhibited the lowest strength loss after exposure to hygrothermal conditions for 3000 h. This behaviour of an unusual trend of bio-epoxy can be attributed to the absence of a hydrolysis reaction with no formation of additional hydroxyl groups as noted in the FTIR analysis. This indicates that only reversible plasticization has played a role in the reduction of the tensile strength, contrary to epoxy and vinyl ester, where both irreversible hydrolysis and reversible plasticization came into effect. Because of only reversible degradation, bio-epoxy has recovered most of its properties after storing in an ambient environment. Although the glass transition temperature has increased after exposure, because of additional cross-linking of polymeric chains caused by rearrangement and reduction of free volume, the tensile strength of resins still decreased. This can be attributed to the role of absorbed moisture that has resulted in degradation of resins in terms of the reversible plasticization and irreversible hydrolysis.

Table 10
Tensile strength of glass fibre yarn and resin systems after hygrothermal conditioning.

Tested Material		Property	Exposure Duration				Retention after 3000 h
			0 hrs	1000 hrs	2000 hrs	3000 hrs	
Fibre Yarn	**Glass**	Tensile Strength (MPa)	1602.38	1314.12	1032.40	1004.18	63.00 %
		SD	47.65	44.54	35.61	40.26	
		CoV (%)	2.97	3.39	3.45	4.01	
Resin systems	**Epoxy**	Tensile Strength (MPa)	62.44	59.94	54.97	50.93	81.56 %
		SD	2.89	2.46	2.40	2.06	
		CoV (%)	4.63	4.11	4.38	4.06	
	Bio-epoxy	Tensile Strength (MPa)	52.32	50.15	49.64	47.24	90.29 %
		SD	1.08	1.90	1.32	0.83	
		CoV (%)	2.00	3.78	2.66	1.75	
	Vinyl Ester	Tensile Strength (MPa)	40.70	46.58	43.21	33.80	83.04 %
		SD	1.87	2.07	1.96	1.62	
		CoV (%)	5.00	4.45	4.54	4.80	

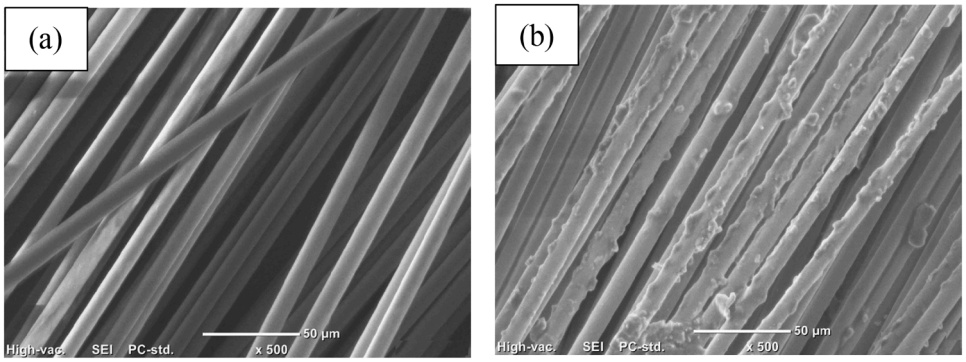

Fig. 8. Morphology of glass fibres (a) unexposed (b) exposed to 3000 hrs.

3.4.3. *Modulus of neat resin*

Hygrothermal exposure has significantly affected the stress-strain behaviour and tensile modulus of all three resins. It can be observed from Table 11 that the strain at failure of bio-epoxy has increased progressively with increasing exposure time, while the modulus gradually decreased and exhibited a decrement of 13.5 % after 3000 hrs. This behaviour of bio-epoxy was observed because the Type-I bound water has induced the plasticization effect. From Table 11, it can be observed that in case of epoxy and vinyl ester resin samples the strains at the failure have decreased significantly after hygrothermal ageing with increasing exposure duration. This declining trend was noticed because of the chemical degradation involving the hydrolysis and the molecular chain scission after prolonged hygrothermal ageing. While the elastic modulus has increased gradually with increasing exposure duration, with an increment of 12.9 % and 11.6 % for epoxy and vinyl ester, respectively, as evident from Table 11. This is because the hygrothermal ageing has caused the secondary cross-linking in the polymeric chains, responsible for increased elastic modulus of the material [48]. Xu et al [49] also documented the same behaviour of epoxy with brittle failure and reduced strain at failure after exposure to a hygrothermal environment at 75 °C for 2530 h. The modulus increased after exposure because additional crosslinking and reduced free volume resulted in a densified network, leading to brittle behaviour with lower strain at failure (*Table 11*). Whereas the tensile strength decreased as prolonged moisture exposure caused reversible plasticization and irreversible hydrolysis of the polymer.

Fig. 9 shows the fracture surfaces of resin samples broken after tensile tests, visualised using SEM. Fig. 9(a) and (b) reveal the fracture morphology of bio-epoxy resin before and after exposure. The fracture surface of the bio-epoxy after hygrothermal ageing exhibited a ductile nature, comprising uniformly spaced stretch lines. Fig. 9(c) and (d) revealed that the epoxy resin has a brittle failure with increased river lines and ridges after exposure. The similar river lines are recognized and reported by other researchers as an indication of brittle failure in polymer composite materials[28]. It can also be noted that the brittle failure of epoxy has induced visible cracks on the fracture surface. Likewise, Fig. 9(e) shows the brittle nature of vinyl ester resin with clear fish scale marks on the surface. Vinyl ester samples have gained severity after exposure, with more rigorous scaling on the fractured surface as shown in Fig. 9(f). These SEM observations of the failure behaviour align with the measured changes in the ductility and elastic modulus of the different resin systems as discussed earlier.

3.5. *Effect of hygrothermal exposure on interfacial shear strength*

The interfacial shear strength of single-yarn composites was calculated by single-yarn fragmentation test following Kelly and Tyson's approach [53]. The formula used for the calculation of IFSS is given below as Eq. (8) [28]:

$$\tau = \frac{F}{L\pi D} \quad \text{(Eq. 8)}$$

Where F represents the maximum load at failure, L corresponds to embedded fibre length in the resin, i.e., 33 mm in this study, and D stands for the diameter of the fibre.

The reduction in interfacial shear strength (IFSS) of single yarn composites after exposure to hygrothermal conditions and the IFSS retention after 3000 h are presented in Table 12. The hygrothermal exposure has negatively affected the interfacial shear strength by damaging the interface between the fibre and resin. Single yarn composites of vinyl ester were most affected by hygrothermal exposure after 3000 h, with a maximum strength loss of 20.5 %, whereas bio-epoxy composites were least affected, with a strength loss of 5.7 %. Epoxy/glass composites also exhibited a declining trend after exposure, with a 13.5 % loss in interfacial shear strength. The reduction in IFSS can be attributed to degradation of interface between fibre and resin caused by micro-cracking and debonding [3]. The most probable reason for the degradation could be a potential route of moisture ingress along the interphase that can be responsible for the hydrolysis of the interphase region [36], thereby reducing the load transfer capabilities. Assarar et al [32] observed a similar degradation mechanism in flax/epoxy and glass/epoxy composites under water ageing. Fibre sizing has an important role in the adhesion between fibre and resin, as it has the capability to react with the matrix and make a chemical bond. But after exposure to a hygrothermal environment, the hydrolysis of Si-O-Si bonding between silane-based sizing on glass fibre and resin matrix might have also

Table 11
Tensile modulus and strain at failure of resin systems before and after exposure.

Resin Type	Property	Exposure Duration				Retention after 3000 hr
		0 hrs	1000 hrs	2000 hrs	3000 hrs	
Epoxy	Modulus (MPa) [SD]	3377 [89]	3579 [77]	3797 [81]	3813 [64]	112.91 %
	Strain at failure (%)	2.74	2.36	2.22	1.86	
Bio-epoxy	Modulus (MPa) [SD]	2972 [72]	2688 [52]	2589 [63]	2569 [68]	86.425
	Strain at failure (%)	3.84	4.24	3.95	4.46	
Vinyl Ester	Modulus (MPa) [SD]	3708 [93]	3850 [84]	4013 [98]	4139 [76]	111.65 %
	Strain at failure (%)	1.51	1.48	1.41	1.20	

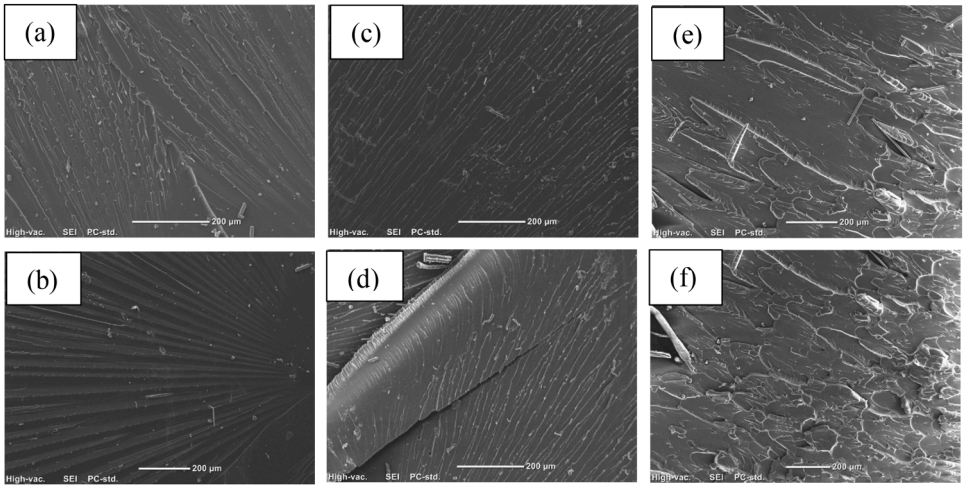

Fig. 9. Fracture morphology (a) bio-epoxy (control), (b) bio-epoxy (exposed), (c) epoxy (control), (d) epoxy (exposed), (e) vinyl ester (control), (f) vinyl ester (exposed).

Table 12
Interfacial shear strength of single-yarn composites with glass fibre and different types of resins and IFSS retention.

Resin Type	Property	Exposure Duration				IFSS retention after 3000 hrs
		0 hrs	1000 hrs	2000 hrs	3000 hrs	
Epoxy	IFSS (MPa)	48.84	43.94	42.70	42.24	86.48 %
	SD	1.55	1.46	1.86	2.24	
	CoV (%)	3.00	3.34	4.36	5.31	
Bio-Epoxy	IFSS (MPa)	45.08	43.26	42.50	41.88	92.90 %
	SD	1.22	1.82	1.16	1.24	
	CoV (%)	3.00	4.21	2.77	2.91	
Vinyl Ester	IFSS (MPa)	29.78	28.01	24.44	23.67	79.48 %
	SD	1.48	1.22	0.48	1.17	
	CoV (%)	5.00	4.39	1.98	4.97	

contributed in the reduction of IFSS [33]. Krauklis et al [15] also confirmed the damage caused to the coupling agent of the sizing-rich interface due to plasticization and hydrolysis after hygrothermal ageing in glass fibre composites.

The results of interfacial shear strength tests revealed that the bio-epoxy/glass composites have the highest strength retention after exposure to hygrothermal condition. The better performance of bio-epoxy than epoxy and vinylester can be because this resin system did not experience hydrolysis, and the reduction in IFSS can only be attributed to the plasticization effect. The water absorbed by bio-epoxy was mostly free Type-I water that is only responsible for the plasticization of resin. Plasticization is a reversible degradation mechanism, so bio-epoxy has reinstated most of the properties once stored at room temperature after removing from the exposure chamber. A similar phenomenon of restoration of the properties of resins after desorption of moisture has been explained by different researchers [17,54]. The other probable reason could be the presence of additional hydroxyl groups due to the glycerol core that enabled bio-epoxy to exhibit strong adhesive properties by forming hydrogen bonding with glass fibres. Contrary to this, degradation of both vinyl ester/glass and epoxy/glass occurred because of the hydrolysis along the interfacial zone, as well as the plasticization, as confirmed by FTIR spectra before and after exposure in Section 3.3. Hydrolysis caused irreversible damage in the interfacial zone of fibre and resins, resulting in the higher IFSS loss. The governing failure mechanism can be identified by comparing the loss in tensile strength and IFSS. In case of vinyl ester/glass composites, IFSS was reduced more than tensile strength, revealing that the fibre/resin interface failure was the dominant degradation mechanism. This is because the resin part in vinyl ester is less affected because of lower moisture absorption, but the hydrolysis of the interfacial zone resulted in excessive debonding and eventually fibre pull-out. In contrast, for epoxy and bio-epoxy composites higher reduction in tensile strength was observed as compared to IFSS, indicating that the failure for these resin systems was matrix dominant.

SEM observations were carried out to reveal the changes in the microstructure of single yarn composites after conditioning. SEM images of the single yarn composites without exposure are displayed in Fig. 10 (a, c, e). Whereas the microstructure of samples exposed to hygrothermal conditioning for 3000 h is evidenced in Fig. 10 (b, d, f). The extent of visible damage in each of the micrographs complements and is in line with the results of IFSS reduction with prolonged exposure presented earlier in Table 12. From all the SEM images, it can be observed that the major failure mechanisms involve the debonding at fibre/resin interface, resin failure, fibre pull-out and breakage. Similar failure mechanisms were also reported by different researchers [27,28].

Fig. 10 (a and b) revealed that after exposure to hygrothermal condition, epoxy/glass composites were damaged due to matrix cracking, fibre pull out, and debonding at interface with matrix failure as the dominant failure mode. Likewise, Fig. 10 (c, d) shows the cross-section of bio-epoxy/glass composite before and after exposure. It can be observed that there is some damage caused by fibre pull-out and debonding, but the dominant failure mechanism was matrix failure. Furthermore, the extent of damage was much lesser compared to epoxy/glass composites, which correlates with the results presented earlier. Lastly, the failure in vinyl ester/glass composites the failure was mainly due to debonding at the interface, leading to excessive fibre breakage and pull out as shown in Fig. 10 (e, f).

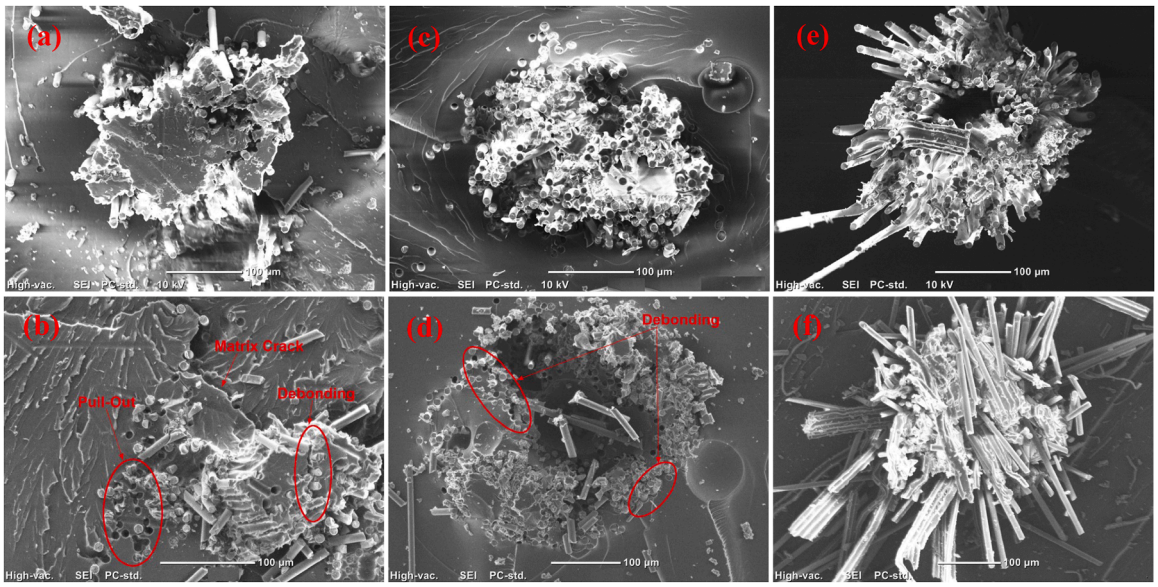

Fig. 10. (a) Epoxy/glass (unexposed), (b) Epoxy/glass (exposed), (c) Bio-epoxy/glass (unexposed), (d) Bio-epoxy/glass (exposed), (e) Vinyl ester/glass (unexposed), (f) Vinyl ester/glass (exposed).

4. Significance of the resin types on the durability using ANOVA

Analysis of variance (ANOVA) was performed for evaluating the effect of resin types on the durability after exposure to hygrothermal conditioning. In two-way ANOVA, resin types and exposure durations were set as two independent variables, whereas the percentage retention of interfacial shear strength, tensile strength, Tg and water absorption were the dependent variables. The results of two-way ANOVA (Table 13) demonstrate that there was a significant effect of resin type and exposure time on tensile strength retention, as the p-value for both is <0.001. This is much less than 0.05 (i.e., 95 % confidence level) with a partial eta square value of 0.52 and 0.68, respectively. Likewise, the resin types and exposure time have a significant effect on the IFSS retention (p-value is <0.05 with R^2 values of 0.31 and 0.24, respectively). Furthermore, the retention of Tg and water absorption was also considerably affected (p-value is <0.05 with R^2 values of 0.99 and 0.86, respectively). It can be inferred from partial eta squared that water absorption and Tg are the most significantly affected properties by varying the resin types. Furthermore, the R^2 values of tensile and IFSS degradation indicated that the resin is more affected than the fibre/matrix interface under a hygrothermal environment.

5. Evaluation of resin performance by analytical hierarchy process

The optimal resin type that can increase the resistance of glass fibre composites against hygrothermal environment was identified by the analytical hierarchy process (AHP), considering the importance of evaluated properties. Saaty and Vargas [55] scale (1–9) was used to express the relative importance of all attributes. A matrix of relative importance, $M = [a_{ij}]_{nxn,}$ expressed by Eq. (9) was constructed for n attributes, where a_{ij} denotes the importance of the i^{th} attribute in relation to the j^{th} attribute.

$$M = \begin{bmatrix} a_{11} & \cdots & a_{1n} \\ \vdots & \ddots & \vdots \\ 1/a_{1n} & \cdots & a_{nn} \end{bmatrix} \quad \text{(Eq. 9)}$$

The normalized Eigen vector of matrix M can be generated by normalizing each value against the sum of all its entries, as expressed in Eq. (10).

$$a_{ij} = \frac{a_{ij}}{\sum_{i=1}^{n} a_{ij}} \quad \text{(Eq. 10)}$$

The consistency ratio (CR) expressed as Eq. (11) should be checked to confirm consistency in relative importance. Only the values with CR ≤ 0.1 were accepted.

$$CR = CI/RI \quad \text{(Eq. 11)}$$

where *CI* is the consistency index that can be determined using Eq. (12) and *RI* represents the random index.

$$CI = \frac{\lambda_{max} - n}{n - 1} \quad \text{(Eq. 12)}$$

5.1. Hierarchy of criteria and sub-criteria

The criteria included aspects including physical, mechanical, thermal, chemical, and microstructural properties, which were prioritized based on their intended purpose during the service life. In total, six scenarios were assessed by varying the priority rankings of physical, thermal, and mechanical properties. The chemical and microstructural properties were assigned with fourth and fifth priorities, respectively, in all cases. *Table 14* presents the one-to-one comparison of criteria on the basis of relative importance and intensities for each case.

Table 15 summarizes the relative importance assigned to sub-criteria. The degree of cure was slightly preferred over glass transition temperature for thermal properties of the resin system, as full curing is important for strength gain, while water absorption was strongly more important than yellowing for physical properties. Tensile strength and

Table 13
Outcome of ANOVA.

Variables		p-value	Effect size (partial η^2)
Dependent	Independent		
Tensile Strength retention	Resin Type	<0.001	0.523
	Exposure Duration	<0.001	0.682
IFSS retention	Resin Type	<0.001	0.317
	Exposure Duration	<0.001	0.242
Retention in Tg	Resin Type	<0.001	0.999
	Exposure Duration	<0.001	0.866
Water absorption	Resin Type	<0.001	1.00
	Exposure Duration	<0.001	1.00

Table 14
Pairwise comparison of criteria.

Pair	Intensity					
	C-1	C-2	C-3	C-4	C-5	C-6
Mechanical vs Physical	7	8	1/2	1/5	3	1/4
Mechanical vs Thermal	6	5	1/3	1/3	4	1/5
Mechanical vs Chemical/ Microstructural	8	8	7	5	8	4
Physical vs Thermal	8	8	7	5	8	4
Physical vs Chemical/Microstructural	4	4	4	5	6	5
Thermal vs Chemical/Microstructural	5	5	5	8	5	5

*Chemical is twice as important as microstructure in all scenarios.

IFSS were ranked as moderately more important than modulus and strain at failure for mechanical properties. However, IFSS was slightly more important than tensile strength, and modulus was slightly more important than strain at failure.

5.2. Determination of the most suitable alternative

Table 16 presents different cases by altering the priorities and the best-performing resin after hygrothermal exposure for all cases, considering the relative significance of each attribute. The selection of the best resin system is mainly dependent on the order of prioritizing its properties, as indicated in Table 16. For instance, in first case (C-1), the mechanical properties were assigned with highest priority, followed by physical and thermal properties. Bio-epoxy was the best-performing resin with the highest priority (%) of 35.61 %, followed by vinyl ester and epoxy with percentage priority of 32.65 % and 31.73 %, respectively. If the end user prioritizes mechanical properties, based on the intended application of the resin system, bio-epoxy could be the best option. Alternatively, if the highest priority was assigned to physical properties, vinyl ester would be preferable. However, if thermal properties are set at the highest priority, the best resin system could be either bio-epoxy or vinyl ester, depending on the relative significance of the physical and mechanical properties.

6. Conclusions

This study evaluated the properties of single yarn glass fibre composites with either epoxy, bio-epoxy, and vinylester resin under a hygrothermal environment. The composites were exposed to 60 °C and 98 % RH for 1000, 2000, and 3000 h. By linking moisture diffusion behaviour, chemical stability, thermal transitions, and mechanical property retention, this work provides a comprehensive assessment of how different resin chemistries respond to prolonged environmental stress. The key results lead to the following conclusions:

Table 15
Pairwise comparison matrix for sub-criteria.

Mian Criteria	Sub-criteria		Relative Importance	Intensity
	A	B		
Mechanical	Tensile strength	IFSS	B	2
	Tensile strength	Modulus	A	3
	Tensile strength	Failure strain	A	3
	IFSS	Modulus	A	3
	IFSS	Failure strain	A	3
	Modulus	Failure strain	A	2
Physical	Water Absorption	Yellowing	A	5
Thermal	Tg	Degree of cure	B	2

1. Bio-epoxy exhibited the highest water absorption amongst the resin types investigated because of the presence of glycerol core with additional hydroxyl groups. Vinyl ester resin was saturated only after 150 h with the highest diffusion coefficient, whereas bio-epoxy and epoxy exhibited relatively lower and comparable diffusion coefficients with full saturation after 2200 and 2500 h, respectively.
2. Hygrothermal exposure can cause significant yellowing regardless of the resin type because of the chromophores. Vinyl ester showed the highest yellowing resistance, followed by epoxy and bio-epoxy, because of its fewer ester linkages sterically shielded by a hydrophobic core, reducing their surface accessibility during exposure.
3. Bio-epoxy and vinyl ester have better thermal stability than epoxy under a hygrothermal environment. The T_g of both these resins remained the same, while the T_g of epoxy resin increased up to 26 % after exposure for 3000 h due to additional cross-linkage in polymeric chains. FTIR revealed no hydrolysis in bio-epoxy after exposure to hygrothermal exposure for 3000 hrs. In contrast, both epoxy and vinyl ester undergo hydrolysis reactions.
4. The least reduction in tensile strength, modulus, and interfacial shear strength was observed when glass fibre yarn was used with bio-epoxy, followed by vinyl ester and epoxy. The higher tensile strength retention of composites made from bio-epoxy resin can be attributed to its strength only affected by plasticization, while both plasticization and hydrolysis adversely affected epoxy and vinyl ester. The dominant failure mode of glass fibre composites from bio-epoxy and epoxy was matrix failure, while it was fibre/matrix debonding for vinyl ester.
5. Two-way ANOVA revealed that the effect of resin types is more prominent on the degradation of tensile properties compared to IFSS degradation, indicating that resin is the more affected constituent material. AHP indicated that under hygrothermal environment, bio-epoxy would be the optimal option if mechanical properties were the highest priority, while vinyl ester could be a suitable option if physical/thermal properties were the highest priority when using glass fibre composites in a hygrothermal environment.

These conclusions correspond to the specific family types of the resin system and the attributes considered for each simulated investigated property. However, the implemented approaches and results provide a framework for the evaluation of the durability of composites with various resin systems exposed to aggressive environments. Furthermore, resins were cured under manufacturer-recommended conditions to reflect standard practice. Although the exposure temperature exceeded the curing temperatures of epoxy and bio-epoxy, the aim was to compare durability under typical manufacturing and service conditions. This research can be extended to other resin and fibre systems to validate the reliability of the developed models and to seek a deeper knowledge of the durability of polymer composites exposed to a hygrothermal environment.

Future recommendations

Further research is recommended to develop a predictive model capable of explaining the unusual high-uptake/low-damage behaviour of bio-epoxy. A systematic investigation about the restoration of the mechanical performance of bio-epoxy after desorption of water would be insightful in understanding the long-term durability of bio-epoxy composites. Furthermore, colour change should be quantified more rigorously by integrating UV–Vis spectroscopy with ASTM E313 yellowing indices.

CRediT authorship contribution statement

Abdullah Iftikhar: Writing – original draft, Visualization, Methodology, Investigation, Formal analysis, Data curation. **Allan Manalo:** Writing – review & editing, Supervision, Project administration,

Table 16
Different priority cases with corresponding best-performing resin.

Case	Order of priorities			% priority			Best Resin
	1st	2nd	3rd	Epoxy	Bio-epoxy	Vinyl ester	
C1	Mechanical	Physical	Thermal	31.73	35.61	32.65	Bio-epoxy
C2	Mechanical	Thermal	Physical	31.90	35.83	32.26	Bio-epoxy
C3	Physical	Mechanical	Thermal	30.42	31.59	37.98	Vinyl ester
C4	Physical	Thermal	Mechanical	30.30	29.46	40.22	Vinyl ester
C5	Thermal	Mechanical	Physical	33.04	34.13	32.82	Bio-epoxy
C6	Thermal	Physical	Mechanical	32.48	32.13	35.38	Viny ester

Funding acquisition, Conceptualization. **Zaneta Senselova:** Writing – review & editing, Validation, Methodology. **Wahid Ferdous:** Writing – review & editing, Supervision. **Mazhar Peerzada:** Writing – review & editing, Investigation. **Hannah Seligmann:** Writing – review & editing, Supervision. **Kate Nguyen:** Writing – review & editing, Funding acquisition. **Brahim Benmokrane:** Writing – review & editing, Funding acquisition.

Declaration of competing interest

The authors declare no competing financial interests or personal relationships that could have influenced this work.

Acknowledgements

The first author acknowledges the financial support, including an RTP stipend, research scholarship and UniSQ International fees scholarship from the University of Southern Queensland for conducting his PhD. The authors acknowledge the financial support from the ARC Discovery Project (DP230101152) on Degradation mechanisms of structural composites under extreme weather, and the Natural Science and Engineering Research Council (NSERC) of Canada. The authors also deeply acknowledge the support from Colan Australia for providing the fibre yarns, Climate Change Pty Ltd. for supplying the bio-epoxy resin and Allnex for supplying vinyl ester resin.

Data availability

Data will be made available on request.

References

[1] A. Manalo, O. Alajarmeh, W. Ferdous, B. Benmokrane, C.D. Sorbello, A. Gerdes, Effect of simulated hygrothermal environment on the flexural and interlaminar shear strength of particulate-filled epoxy-coated GFRP composites, Constr. Build. Mater. 339 (2022), https://doi.org/10.1016/j.conbuildmat.2022.127687.
[2] S. Ishtiaq, M.Q. Saleem, R. Naveed, M. Harris, S.A. Khan, Glass–Carbon–Kevlar fiber reinforced hybrid polymer composite (HPC): part (A) mechanical and thermal characterization for high GSM laminates, Compos. C 14 (2024), https://doi.org/10.1016/j.jcomc.2024.100468.
[3] I.R. Chowdhury, P.S. Rao, N.P. O'Dowd, A.J Comer, Hygrothermal ageing effects on failure behaviour of fibre-reinforced polymer composite materials under in-situ SEM testing, Compos. B. Eng. 294 (2025), https://doi.org/10.1016/j.compositesb.2025.112148.
[4] A. Sharda, A. Manalo, W. Ferdous, Y. Bai, L. Nicol, A. Mohammed, et al., Axial compression behaviour of all-composite modular wall system, Compos. Struct. 268 (2021) 113986, https://doi.org/10.1016/j.compstruct.2021.113986.
[5] W. Ferdous, A. Manalo, O. AlAjarmeh, A.A. Mohammed, C. Salih, P. Yu, et al., Static behaviour of glass fibre reinforced novel composite sleepers for mainline railway track, Eng. Struct. 229 (2021) 111627, https://doi.org/10.1016/j.engstruct.2020.111627.
[6] R.M. Hizam, A.C. Manalo, W. Karunasena, Y. Bai, Behaviour of pultruded GFRP truss system connected using through-bolt with mechanical insert, Compos. B. Eng. 168 (2019) 44–57, https://doi.org/10.1016/j.compositesb.2018.12.052.
[7] J.R. Pothnis, A. Hejjaji, G.S. Bhatia, A. Comer, Failure analysis under fatigue loading of glass fibre reinforced in-situ polymerizable thermoplastic and Bio-epoxy based composites, Compos. C 17 (2025), https://doi.org/10.1016/j.jcomc.2025.100608.
[8] A. Robin, M. Arhant, P. Davies, S. Lejeune, E. Lolive, T. Bonnemains, et al., Effect of aging on the in-plane and out-of-plane mechanical properties of composites for design of marine structures, Compos. C 11 (2023), https://doi.org/10.1016/j.jcomc.2023.100354.
[9] A.C. Manalo, O. Alajarmeh, D. Cooper, C.D. Sorbello, S.Z. Weerakoon, B. Benmokrane, Manufacturing and structural performance of glass-fiber-reinforced precast-concrete boat ramp planks, Structures 28 (2020) 37–56, https://doi.org/10.1016/j.istruc.2020.08.041.
[10] B. Benmokrane, A.H. Ali, H.M. Mohamed, A. ElSafty, A. Manalo, Laboratory assessment and durability performance of vinyl-ester, polyester, and epoxy glass-FRP bars for concrete structures, Compos. B. Eng. 114 (2017) 163–174, https://doi.org/10.1016/j.compositesb.2017.02.002.
[11] D. Gibhardt, A.E. Krauklis, A. Doblies, A. Gagani, A. Sabalina, O. Starkova, et al., Time, temperature and water aging failure envelope of thermoset polymers, Polym. Test. 118 (2023) 107901, https://doi.org/10.1016/j.polymertesting.2022.107901.
[12] O.H. Margoto, A.S. Milani, Comparing flax fibre/biopolymer woven composites with carbon fibre-enhanced, partially green alternatives: mechanical performance versus sustainability, Compos. C 16 (2025), https://doi.org/10.1016/j.jcomc.2024.100547.
[13] N. Vellguth, M. Shamsuyeva, H.J. Endres, F. Renz, Accelerated ageing of surface modified flax fiber reinforced composites, Compos. C 6 (2021), https://doi.org/10.1016/j.jcomc.2021.100198.
[14] C.S. Sirimanna, M.M. Islam, T. Aravinthan, Temperature effects on full scale FRP bridge using innovative composite components, in: L. Ye, P. Feng, Q. Yue (Eds.), Advances in FRP Composites in Civil Engineering, Springer Berlin Heidelberg, Berlin, Heidelberg, 2011, pp. 376–380, https://doi.org/10.1007/978-3-642-17487-2_82.
[15] A.E. Krauklis, O. Starkova, D. Gibhardt, G. Kalinka, H.A. Aouissi, J. Burlakovs, et al., Reversible and irreversible effects on the epoxy GFRP fiber-matrix interphase due to hydrothermal aging, Compos. C 12 (2023), https://doi.org/10.1016/j.jcomc.2023.100395.
[16] K. Mishra, A. Singh, Time-dependant degradation of highly cross-linked epoxy due to hygrothermal ageing at three different temperatures, Polym. Degrad. Stab. 215 (2023), https://doi.org/10.1016/j.polymdegradstab.2023.110448.
[17] R. Guo, G. Xian, C. Li, B. Hong, X. Huang, M. Xin, et al., Water uptake and interfacial shear strength of carbon/glass fiber hybrid composite rods under hygrothermal environments: effects of hybrid modes, Polym. Degrad. Stab. 193 (2021), https://doi.org/10.1016/j.polymdegradstab.2021.109723.
[18] M.M. Khotbehsara, A. Manalo, T. Aravinthan, K.R. Reddy, W. Ferdous, H. Wong, et al., Effect of elevated in-service temperature on the mechanical properties and microstructure of particulate-filled epoxy polymers, Polym. Degrad. Stab. 170 (2019), https://doi.org/10.1016/j.polymdegradstab.2019.108994.
[19] A. Manalo, G. Maranan, S. Sharma, W. Karunasena, Y. Bai, Temperature-sensitive mechanical properties of GFRP composites in longitudinal and transverse directions: a comparative study, Compos. Struct. 173 (2017) 255–267, https://doi.org/10.1016/j.compstruct.2017.04.040.
[20] G. Hota, W. Barker, A. Manalo, Degradation mechanism of glass fiber/vinylester-based composite materials under accelerated and natural aging, Constr. Build. Mater. 256 (2020), https://doi.org/10.1016/j.conbuildmat.2020.119462.
[21] Z. Lu, M. Jiang, Y. Pan, G. Xian, M. Yang, Durability of basalt fibers, glass fibers, and their reinforced polymer composites in artificial seawater, Polym. Compos. 43 (2022) 1961–1973, https://doi.org/10.1002/pc.26511.
[22] Z. Zhang, Q. Ji, Z. Guo, C. Li, R. Guo, J. Tian, et al., Design, preparation, and mechanical properties of glass fiber reinforced thermoplastic self-anchor plate cable exposed in alkaline solution environment, Polym. Compos. 45 (2024) 11687–11700, https://doi.org/10.1002/pc.28591.
[23] M.M. Khotbehsara, A. Manalo, T. Aravinthan, W. Ferdous, K.T.Q. Nguyen, G. Hota, Ageing of particulate-filled epoxy resin under hygrothermal conditions, Constr. Build. Mater. 249 (2020), https://doi.org/10.1016/j.conbuildmat.2020.118846.
[24] D. Scida, M. Assarar, C. Poilâne, R. Ayad, Influence of hygrothermal ageing on the damage mechanisms of flax-fibre reinforced epoxy composite, Compos. B. Eng. 48 (2013) 51–58, https://doi.org/10.1016/j.compositesb.2012.12.010.
[25] B.C. Ray, Temperature effect during humid ageing on interfaces of glass and carbon fibers reinforced epoxy composites, J. Colloid. Interface. Sci. 298 (2006) 111–117, https://doi.org/10.1016/j.jcis.2005.12.023.
[26] A.M. Elarbi, H.C. Wu, Flexural behavior of epoxy under accelerated hygrothermal conditions, Fibers 5 (2017), https://doi.org/10.3390/fib5030025.
[27] M.C. Seghini, F. Touchard, F. Sarasini, L. Chocinski-Arnault, D. Mellier, J. Tirillò, Interfacial adhesion assessment in flax/epoxy and in flax/vinylester composites by single yarn fragmentation test: correlation with micro-CT analysis, Compos. Appl. Sci. Manuf. 113 (2018) 66–75, https://doi.org/10.1016/j.compositesa.2018.07.015.

[28] Z. Khan, B.F. Yousif, M. Islam, Fracture behaviour of bamboo fiber reinforced epoxy composites, Compos. B. Eng 116 (2017) 186–199, https://doi.org/10.1016/j.compositesb.2017.02.015.
[29] R. Livingston, B. Koohbor, Characterizing fiber-matrix debond and fiber interaction mechanisms by full-field measurements, Compos. C 7 (2022), https://doi.org/10.1016/j.jcomc.2022.100229.
[30] J.H.S. Almeida, S.D.B. Souza, E.C. Botelho, S.C. Amico, Carbon fiber-reinforced epoxy filament-wound composite laminates exposed to hygrothermal conditioning, J. Mater. Sci. 51 (2016) 4697–4708, https://doi.org/10.1007/s10853-016-9787-9.
[31] A. Moudood, A. Rahman, H.M. Khanlou, W. Hall, A. Öchsner, G. Francucci, Environmental effects on the durability and the mechanical performance of flax fiber/bio-epoxy composites, Compos. B. Eng. 171 (2019) 284–293, https://doi.org/10.1016/j.compositesb.2019.05.032.
[32] M. Assarar, D. Scida, A. El Mahi, C. Poilâne, R. Ayad, Influence of water ageing on mechanical properties and damage events of two reinforced composite materials: flax-fibres and glass-fibres, Mater. Des. 32 (2011) 788–795, https://doi.org/10.1016/j.matdes.2010.07.024.
[33] M. Nikforooz, L. Daelemans, K. De Clerck, W. Van Paepegem, The effect of hydrothermal ageing on the interfacial bonding of E-glass fibre/epoxy in quasi-static and fatigue loading, Compos. B. Eng. 304 (2025) 112649, https://doi.org/10.1016/j.compositesb.2025.112649.
[34] Y. Zhong, M. Cheng, X. Zhang, H. Hu, D. Cao, S. Li, Hygrothermal durability of glass and carbon fiber reinforced composites – a comparative study, Compos. Struct. 211 (2019) 134–143, https://doi.org/10.1016/j.compstruct.2018.12.034.
[35] S. Dong, X. Wu, X. Qi, C. Affolter, G.P. Terrasi, G. Xian, Prediction model of long-term tensile strength of glass fiber reinforced polymer bars exposed to alkaline solution based on Bayesian optimized artificial neural network, Constr. Build. Mater. 400 (2023), https://doi.org/10.1016/j.conbuildmat.2023.132885.
[36] X. Zhuang, J. Ma, Y. Dan, L. Jiang, Y. Huang, Hydrothermal aging of carbon fiber reinforced epoxy composites with different interface structures, Polym. Degrad. Stab. 212 (2023), https://doi.org/10.1016/j.polymdegradstab.2023.110352.
[37] Test method for water absorption of plastics 2022. https://doi.org/10.1520/D0570-22.
[38] Test method for tensile strength and youngs modulus of fibers 2020. https://doi.org/10.1520/C1557-20.
[39] Test method for tensile properties of plastics 2022. https://doi.org/10.1520/D0638-22.
[40] Test method for transition temperatures and enthalpies of fusion and crystallization of polymers by differential scanning calorimetry 2021. https://doi.org/10.1520/D3418-21.
[41] G. Xian, Y. Niu, X. Qi, J. Tian, C. Li, Q. Yue, et al., Water absorption and property evolution of epoxy resin under hygrothermal environment, J. Mater. Res. Technol. 31 (2024) 3982–3997, https://doi.org/10.1016/j.jmrt.2024.07.123.
[42] K. Cheour, M. Assarar, D. Scida, R. Ayad, X.-L. Gong, Effect of water ageing on the mechanical and damping properties of flax-fibre reinforced composite materials, Compos. Struct. 152 (2016) 259–266, https://doi.org/10.1016/j.compstruct.2016.05.045.
[43] Shen Chi-Hung, Springer George S, Moisture absorption and desorption of composite materials, J. Compos. Mater. 10 (1976) 2–20, https://doi.org/10.1177/002199837601000101.
[44] Practice for calculating yellowness and whiteness indices from instrumentally measured color coordinates 2015. https://doi.org/10.1520/E0313-15.
[45] C. Wu, B.C. Meng, Tam L ho, L. He, Yellowing mechanisms of epoxy and vinyl ester resins under thermal, UV and natural aging conditions and protection methods, Polym. Test 114 (2022), https://doi.org/10.1016/j.polymertesting.2022.107708.
[46] A.E. Krauklis, A.T. Echtermeyer, Mechanism of yellowing: carbonyl formation during hygrothermal aging in a common amine epoxy, Polymers 10 (2018), https://doi.org/10.3390/polym10091017.
[47] N. Fereshteh-Saniee, N. Reynolds, C.A. Kelly, P.R. Wilson, M.J. Jenkins, K. N. Kendall, Introducing cryomilling for reliable determination of resin content and degree of cure in structural carbon fibre reinforced thermoset composites, Compos. Appl. Sci. Manuf. 107 (2018) 197–204, https://doi.org/10.1016/j.compositesa.2018.01.004.
[48] J. Zhou, J.P. Lucas, Hygrothermal effects of epoxy resin. Part II: variations of glass transition temperature, Polymer 40 (1999) 5513–5522, https://doi.org/10.1016/S0032-3861(98)00791-5.
[49] K. Xu, W. Chen, X. Zhu, L. Liu, Z. Zhao, G. Luo, Chemical, mechanical and morphological investigation on the hygrothermal aging mechanism of a toughened epoxy, Polym. Test 110 (2022) 107548, https://doi.org/10.1016/j.polymertesting.2022.107548.
[50] Aziz T., Fan H., Khan F.U., Ullah R., Haq F., Iqbal M., et al. Synthesis of carboxymethyl starch-bio-based epoxy resin and their impact on mechanical Properties 2020;234:1759–69. 10.1515/zpch-2019-1434.
[51] J.L. Thomason, L. Yang, R. Meier, The properties of glass fibres after conditioning at composite recycling temperatures, Compos. Appl. Sci. Manuf. 61 (2014) 201–208, https://doi.org/10.1016/j.compositesa.2014.03.001.
[52] D.K. Don, J. Reiner, M. Jennings, M. Subhani, Basalt fibre-reinforced polymer laminates with eco-friendly bio resin: a comparative study of mechanical and fracture properties, Polymers 16 (2024), https://doi.org/10.3390/polym16142056.
[53] A. Kelly, W.R. Tyson, Tensile properties of fibre-reinforced metals: copper/tungsten and copper/molybdenum, J. Mech. Phys. Solids. 13 (1965) 329–350, https://doi.org/10.1016/0022-5096(65)90035-9.
[54] H. Ventura, J. Claramunt, M.A. Rodríguez-Pérez, M. Ardanuy, Effects of hydrothermal aging on the water uptake and tensile properties of PHB/flax fabric biocomposites, Polym. Degrad. Stab. 142 (2017) 129–138, https://doi.org/10.1016/j.polymdegradstab.2017.06.003.
[55] T.L. Saaty, L.G Vargas, Models, Methods, Concepts & Applications of the Analytic Hierarchy Process, 175, Springer US, Boston, MA, 2012, https://doi.org/10.1007/978-1-4614-3597-6.